Mass biases in exclusive radiative hadronic decays of W bosons at the LHC

To cite this article before publication: Eleanor Jones *et al* 2021 *New J. Phys.* in press https://doi.org/10.1088/1367-2630/ac3572

Mass biases in exclusive radiative hadronic decays of W bosons at the LHC

E. Jones[1] **and W. J. Murray**[1&2]

[1]Department of Physics, University of Warwick,
Coventry, CV4 7AL, United Kingdom
[2]STFC, RAL,
Harwell Campus, Didcot, OX11 0QX, United Kingdom

E-mail: eleanor.jones@cern.ch, bill.murray@cern.ch

Abstract. The search for exclusive hadronic vector boson decays is an ongoing part of the LHC programme where, to date, no such decays have been observed. In addition to the intrinsic interest in the branching ratios, there is potential for a measurement of the W boson mass quite distinct from the usual methods. The radiative decay modes offer good potential channels for this search; however, we highlight three issues with it not previously discussed: particle misidentification, partial reconstruction and the impact of interference with QCD. These issues cause shifts in the peak position of tens or hundreds of MeV/c^2.

1. Introduction

Exclusive decays of W and Z bosons to hadronic final states have never been observed. Low-multiplicity final states could potentially be experimentally accessible and, in particular, radiative decays of vector bosons are promising channels with many theoretical predictions of the branching ratios available [1, 2, 3, 4, 5]. However, there is not universal agreement between these predictions. For example, the $W^{\pm}\to\pi^{\pm}\gamma$ branching ratio is estimated to be of the order of 10^{-9} in Ref. [1] and Ref. [4], whereas Ref. [5] proposes values as high as 10^{-7}.

There are experimental limits on many two-body Z decays. These include radiative decays to final states such as $\pi^0\gamma$ [6], $\eta\gamma$ and $\eta'\gamma$ [7], $\omega\gamma$ [8], $\phi\gamma$ [9], $J/\psi\gamma$ and $\Upsilon\gamma$ [10], as well as non-radiative modes such as $\pi^0\pi^0$ [6]. There are fewer experimental limits on similar W decays, although limits on $W^{\pm}\to\pi^{\pm}\gamma$ at 1.50×10^{-5} have been published recently by CMS [11]. The analysis uses W bosons produced in $t\bar{t}$ events, with a leptonically-decaying W boson used to trigger and reduce backgrounds, whilst the other W boson is used for the decay search. The use of this trigger strategy comes at the cost of ignoring inclusive W bosons, but given that the total LHC W cross-section is much larger, approximately 175 nb at 13 TeV according to DYNNLO 1.5 [12, 13], over 5×10^{11} W bosons are expected at the HL-LHC. Therefore, with a suitable trigger, this presents an interesting opportunity and might allow for a W mass measurement to be possible, a measurement previously discarded on grounds of rate in $t\bar{t}$ by Ref. [4].

The current world average mass of the W boson is 80.379 ± 0.012 GeV/c^2 [14]. This is calculated from a combination of results using $p\bar{p}$, e^+e^- and pp interactions at a variety of experiments. There are ongoing studies at the LHC in pp interactions, where the W boson mass is computed from the reconstructed transverse mass using the leptonic decay modes. Precision measurements of the properties of the W boson, including its mass, are essential in testing the predictions of the Standard Model.

ATLAS has demonstrated a dedicated trigger for two-body radiative Z/H decays [9, 15]. It was used in 2015 to select $\phi\gamma$ candidates and was extended in 2016 to include $\rho\gamma$ candidates. It required a 35 GeV E_T photon and a pair of charged tracks consistent with the mass hypothesis studied, giving an efficiency at or above 75%. We assume that a similar strategy, probably requiring a 'τ-candidate' and a photon with a selection on the mass of the pair or the $\mathrm{p_T}$ balance, could be employed for one- and three-track, radiative W boson decay modes. It may also be possible to record exclusive fully-hadronic events using either a J/ψ decaying to muons or a modified tau-pair trigger at first level, with a tight selection on the mass in charged particles at high level, but we focus on the radiative decay topology here.

The ATLAS and CMS detectors at the LHC achieve excellent mass resolution for decays to charged particles and isolated photons, with 1-2 GeV/c^2 quoted by CMS for $H\to\gamma\gamma$ and $H\to ZZ$ [16]. A nominal 1% resolution is used in this paper for decays to such particles. This resolution, combined with the possibility of millions of signal events, suggests a measurement of the W boson mass could be feasible if there are

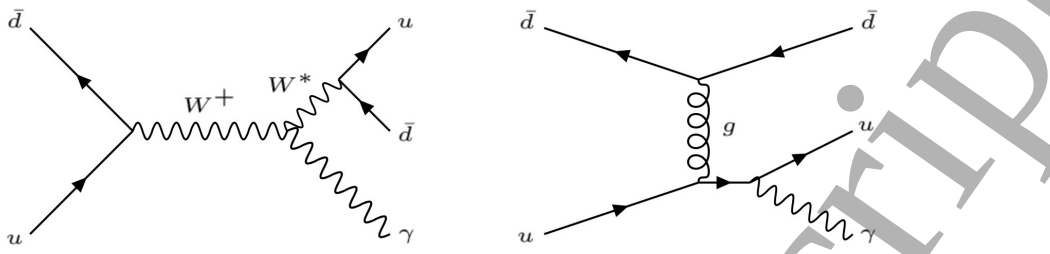

Figure 1. Feynman diagrams demonstrating two processes that have a $u\bar{d}$ pair recoiling against a photon in the final state. The left diagram shows the EW radiative process of interest, whilst the right shows an example QCD process that will lead to interference.

exclusive decay modes with a branching ratio close to the CMS limit above. This paper highlights previously undiscussed issues due to particle (mis)identification, partial reconstruction and EW-QCD interference, which would complicate a mass measurement and require an evaluation, even when simply searching for the decays. Unfortunately, the fragmentation models in Sherpa and PYTHIA are not capable of simulating the two-body $W^{\pm}\to h^{\pm}\gamma$ process, so the paper focusses on $W^{\pm}\to(h^{-}h^{+}h^{\pm})\gamma$, the lowest-multiplicity radiative process where the isolated photon and the charged particle tracks can all be well measured in LHC detectors.

2. Simulating radiative decays

The signature studied here is that of a W boson decaying to a photon recoiling against a low-multiplicity jet. An example Feynman diagram for this process is given in figure 1 (a). For most of the studies, we generate the inclusive process, $W^{+}\to u\bar{d}$ and focus on the decays with a hard photon in the final state, comparing the decay multiplicity for PYTHIA8 [17, 18] and several different Sherpa 2.2.10 configurations [19, 20, 21]. The default Sherpa cluster fragmentation model is not expected to be reliable [F.Krauss, Personal communication] for processes with few particles in the final state, due to a mass of approximately 300 MeV/c^2 assigned to the quarks. Consequently, the Lund string fragmentation model is used for all alternative Sherpa configurations. This is done using the tune parameters suggested in the Sherpa manual: `PARJ(21)=0.432; PARJ(41)=1.05; PARJ(42)=1.0; PARJ(47)=0.65; MSTJ(11)=5`. An alternate tune [22], produced no significant changes in the context of the work presented here. Two-body radiative states cannot be produced by the Lund hadronization model, as the minimum string energy is too great to make only one particle.

The Sherpa configurations tested are: replacing the cluster fragmentation with the Lund string fragmentation (Sherpa-Lund); additionally enabling EW emission (including photons) in the shower using the switch `CSS_EW_MODE=1` (Sherpa-EW-Lund); and, lastly, using the hard matrix element to simulate $W^{+}\to u\bar{d}\gamma$ (Sherpa-ME-Lund). This final configuration is done without the EW emission in the shower enabled to

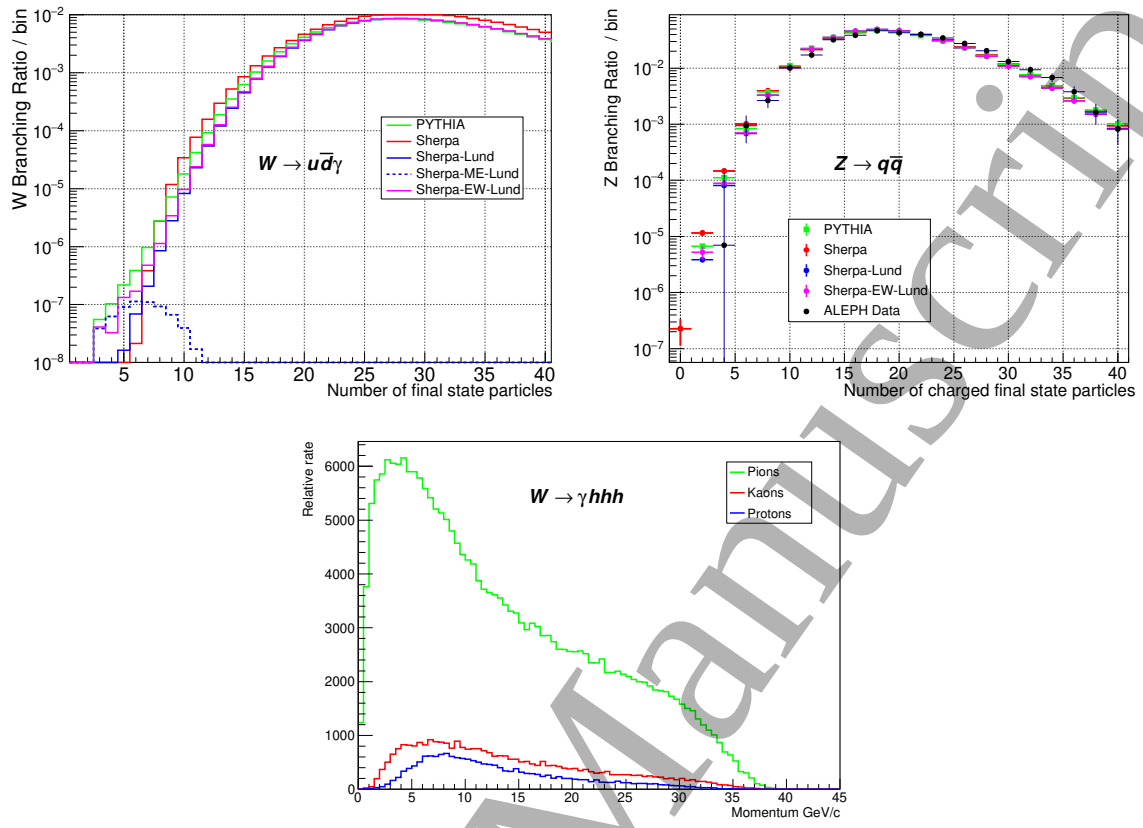

Figure 2. (a) shows the particle multiplicity for the process $W \to u\bar{d}\gamma$, with at least one photon in the final state. (b) shows the charged-particle multiplicity for the process $Z \to q\bar{q}$, with data from the ALEPH experiment overlaid. In these subfigures, PYTHIA is shown in green, and the predictions by the various Sherpa configurations are: default Sherpa (red), Sherpa-Lund (blue), Sherpa-EW-Lund (magenta) and Sherpa-ME-Lund (dashed blue, only shown for $W \to u\bar{d}\gamma$). (c) shows the p_T distribution of the final state particles when requiring a photon and exactly three additional particles, generated using the Sherpa-EW-Lund configuration.

avoid double counting. The decays of π^0s and K^0s are disabled when counting particle multiplicity.

The distributions of the $W^+ \to u\bar{d}$ particle multiplicities produced by these generators when requiring at least one photon in the final state are shown in figure 2 (a). The Sherpa-ME-Lund distribution required a photon energy above 30 GeV and the mass of the $u\bar{d}$ system to be below 20 GeV/c^2. Therefore, this setup can only be expected to be accurate in the extreme low-multiplicity regime. However, as the cross-section is four orders of magnitude lower in this regime, it can be much more efficiently simulated. In addition, with this configuration, both of the diagrams in figure 1 can be produced coherently, allowing the study of interference effects, as discussed in Section 5.

The default Sherpa cluster fragmentation has, overall, the highest branching ratio to at least one photon, which is mostly due to a higher production rate of η mesons. At a multiplicity of ten, the predicted branching ratios (excluding the Sherpa-ME-Lund configuration) span a factor of five, with the largest differences being between the default

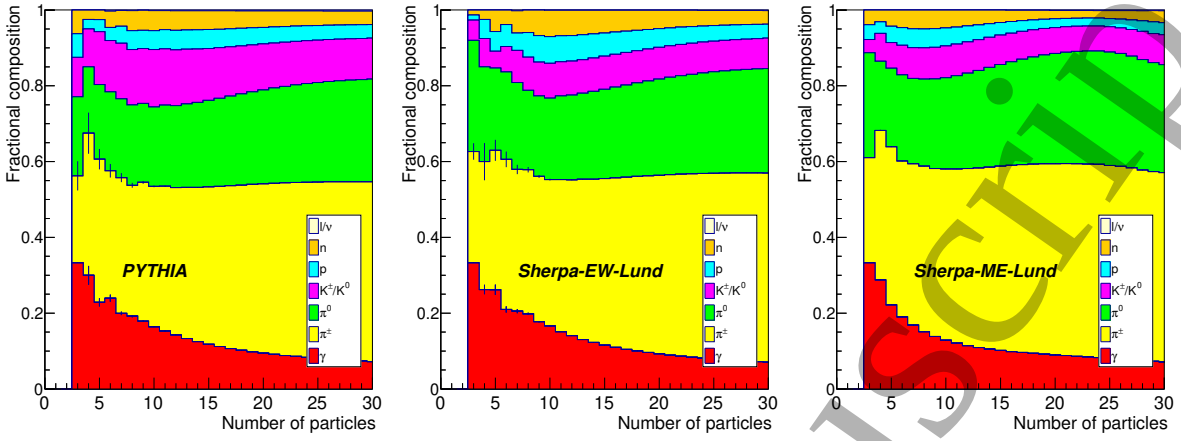

Figure 3. The fractions of leptons, neutrons, protons, kaons, π^0, $\pi^\pm$ and photons predicted by (a) PYTHIA, (b) Sherpa-EW-Lund and (c) Sherpa-ME-Lund for $W^+ \to u\bar{d}$ decays with at least one photon in the final state. Error bars at the top of the photon and charged pion components represent the error on that fraction alone; they are not shown on the other components to reduce clutter.

Sherpa and the Sherpa-Lund configurations. However, at a multiplicity of 5 and below, PYTHIA, Sherpa-EW-Lund and Sherpa-ME-Lund, the only models producing hard photons, are within a factor of three of each other. This approximate agreement supports the use of the matrix-element approach for this extreme phase space. Sherpa-ME-Lund predicts a W branching ratio to a radiative three-body state of $(4.1 \pm 0.2) \times 10^{-8}$, with the other simulations compatible within larger statistical errors.

In figure 2 (b), we show the charged-particle multiplicity for the process $Z \to q\bar{q}$ for the same configurations outlined above. In addition, we overlay data from the ALEPH experiment [23]. The data does not disfavour any of the models and, at charged multiplicities of four or less, is not precise enough to be a definitive guide, though it hints that the true rate of extremely low-multiplicity events could be lower than these simulations predict. One interesting feature is that Sherpa, using its default cluster fragmentation, has the highest probability of producing fewer than five *charged* particles in Z decay, while it has the lowest probability of giving fewer than five *total* particles in radiative W decay. This remains true when the requirement for at least one photon is removed. This emphasises the uncertain nature of these distributions.

3. Particle misidentification

The particle composition of low-multiplicity events predicted by the generators is shown in figure 3, where at least one photon is required from all configurations. There are significant discrepancies in the low-multiplicity region where little data guidance is available. The most extreme example is the kaon fraction, which PYTHIA predicts to be roughly double that predicted by the other models. The statistical precision is much better in the Sherpa-ME-Lund sample, since it was generated with a low-mass

hadronic system that allows for more efficient simulation; however, its predictions at high-multiplicity are not generally applicable.

Consequently, there is considerable uncertainty about the composition of low-multiplicity states and both ATLAS and CMS are not able to reliably distinguish hadron species at these momenta. If the wrong species of particle is attributed to a decay, the estimated boson mass will change. For example, if $W^+ \to p\bar{p}\pi^+\gamma$ is mistaken for $W^+ \to \pi^+\pi^-\pi^+\gamma$, the shift in the peak position of the W boson mass is of the order 60 MeV/c^2. In decays which require a photon and three charged particles in the final state simulated by Sherpa-EW-Lund, the mean shift arising from misidentification is 19 MeV/c^2. This comes from 88 MeV/c^2 in the $pp\pi$ state and 22 MeV/c^2 in the $KK\pi$ state.

The p_T distribution of the final state particles in four-particle events is shown in figure 2 (c). It shows that to distinguish between pions, kaons and protons, the experiments would need good sensitivity up to at least 10 GeV/c. Currently, the LHC detectors have some capability of using $\frac{dE}{dx}$ from the silicon tracker to separate hadrons; however, even at the better performing CMS detector, it has very little power for proton-pion separation above about 3 GeV/c [24].

Both CMS and ATLAS have proposed plans to include timing detectors as part of the Phase II upgrades, primarily to target the challenges that will arise from increased pile-up at the HL-LHC [25, 26]. The time difference between a proton and a pion with a momentum of 15 GeV/c after travelling one meter is 6 ps, well below the 30 ps resolution targets of the timing detectors. Therefore, the addition of these timing detectors will not affect the ability of the experiments to distinguish hadrons in these low-multiplicity decays and, although having the smallest effect on the peak position of the W boson of those studied here, particle misidentification will remain an important factor to consider.

4. Partial reconstruction

Partial reconstruction refers to attempting to reconstruct a particle using a subset of the actual decay products. The example of reconstructing a W^- boson using three charged tracks and a hard photon in the final state, $W^- \to h^-h^+h^-\gamma$, as predicted by Sherpa-ME-Lund, is shown in figure 4, where $h^\pm$ refers to a charged hadron.

The relatively large number of decays including additional neutral particles constitutes a major background that overlaps with the W mass peak. A detector resolution of 1% is assumed, but even with perfect resolution this overlap would be unavoidable due to the W width. These partially reconstructed events could, in principle, be suppressed by vetoing on photon-like calorimeter energy deposits. ATLAS and CMS used 3 GeV and 1 GeV thresholds, respectively, for accepting energy clusters in their electromagnetic calorimeters late in the LHC Run 2 [27, 28]. A π^0 with energy above 2 GeV will give rise to at least one photon with energy above 1 GeV, which suggests it might be possible that they could be efficiently vetoed in the CMS experiment. The effect of vetoing events with a π^0 above this energy is shown in Fig 4 (b).

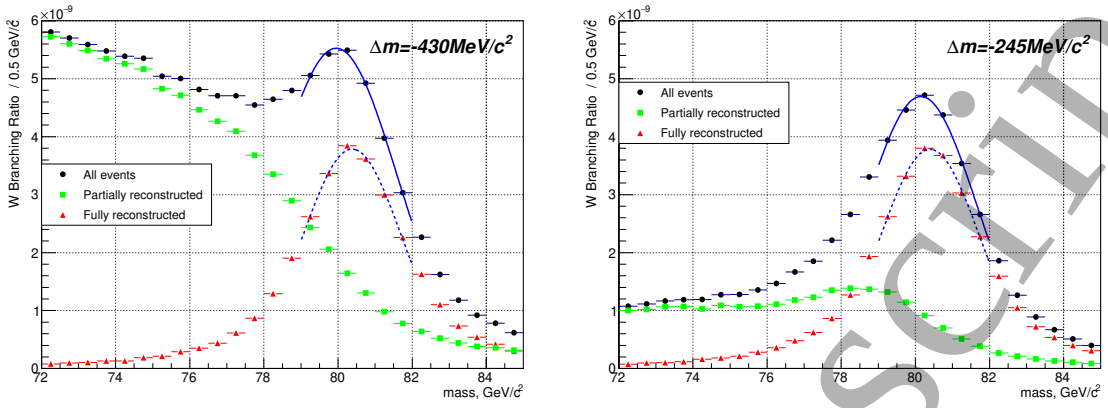

Figure 4. Left: The mass distribution predicted by Sherpa-ME-Lund for a W boson decaying to a photon and three charged tracks. The fully-reconstructed events are in red, whilst those with additional neutral particles are shown in green and the total in black. A detector resolution of 1% is assumed. Right: the same distribution, except with a veto on π^0s with energy over 2 GeV applied. The mass region 79–82 GeV/c^2 is fit with a Gaussian to extract the peak position and the fitted curve is shown in blue.

Although a large fraction of the partially reconstructed decays is removed, the veto is much less efficient close to the W peak. A full fit of the distributions would require knowledge of the rate and mass spectrum of the partially reconstructed events. Instead, the impact on the peak position is quantified by fitting a simple Gaussian to that region, which finds that the measured position is shifted by -430 ± 14 MeV/c^2, or -245 ± 12 MeV/c^2 when the high-momentum π^0 veto is applied. The observed shift, when applying a veto, would depend upon the detailed calorimeter performance under intense pileup and, therefore, it would also have additional systematic errors.

The partially reconstructed event rate could perhaps be measured by reconstructing an additional π^0, although the mix of charged and neutral energy in the jet would degrade the resolution. Alternatively, it is conceivable that information about non-resonant decays could be learnt from the data. However, in each case a reliable model is needed to relate the measured region to the unmeasurable, but most relevant, low momentum π^0s.

Although it was not possible to simulate $W^-\to\pi^-\gamma$ or $W^+\to D_s^+\gamma$, they will also suffer from partial reconstruction due to the $W^-\to\rho^-\gamma$ and $W^+\to D_s^{+*}\gamma$ decays. This is particularly problematic in the case of the D_s^{+*}, where the dominant $D_s^{+*}\to D_s^+\gamma$ decay produces a single photon of low energy.

5. EW-QCD interference

Interference of the hadronic vector boson decay with the t-channel $q\bar{q}\to q\bar{q}$ QCD background has been shown to introduce an apparent reduction in the mass of the peak [29, 30, 31, 32]. This comes from the change in sign of the Breit-Wigner resonance at the peak, overlaid on a continuous QCD background. The effects reported are mass shifts of hundreds of MeV/c^2.

For radiative final states, the Leading Order (LO) Sherpa-ME-Lund setup is used, with the hadronization omitted to speed computation. For these interference studies, all final state particles were required to satisfy $|\eta| < 2.5$, with the mass of the $u\bar{d}$ system required to be below 2 GeV/c^2 and that of the $u\bar{d}\gamma$ system to be between 70 and 90 GeV/c^2. Figure 5 shows the mass predicted by this configuration for $W^+ \to u\bar{d}\gamma$ events from the EW process alone, from the QCD background process and from the coherent sum. The predicted shift in the mass peak is -355 ± 24 MeV/c^2, after including the detector resolution of 1%. The mass shift in $W^- \to d\bar{u}\gamma$ is -322 ± 24 MeV/c^2, consistent with the W^+ but smaller, as expected with a slightly better signal-to-background ratio.

The observed shifts are insensitive to the mass selection applied in the simulation of the di-quark system; increasing the cut on the mass of the $u\bar{d}$ system from 2 to 6 GeV/c^2 made no statistically significant difference. The shifts do, however, depend upon the fiducial region chosen, with the $|\Delta\eta|$ between the hadronic system and the photon very important. They need to be evaluated for each specific experimental configuration. It must also be emphasised that these calculations are at LO only. Thus, they are merely indicative of the scale of the effect and an NLO evaluation would be highly desirable. The observed shifts would be much smaller for W from top decay, since the intrinsic signal-to-background ratio is much better.

The second-generation decays, $W^+ \to c\bar{s}\gamma$ and $W^- \to s\bar{c}\gamma$, have smaller QCD contributions and hence reduced interference. The shifts in the peak positions are consistent with each other, -96 ± 14 MeV/c^2 and -90 ± 48 MeV/c^2, respectively. In addition, an exploration of interference in the fully-hadronic decay mode was conducted. The final state $u\bar{s}s\bar{d}$ was simulated, with all four quarks having a momentum over 2 GeV/c, the $u\bar{s}$ and $s\bar{d}$ systems each required to have a mass below 6 GeV/c^2 and the four other quark pairings having a mass above 10 GeV/c^2. As before, all quarks were required to satisfy $|\eta| < 2.5$. This channel was chosen since it arises naturally in W^+ decay and the quarks are all distinct, which simplifies the simulated phase space definition. The EW signal cross-section, within this (arbitrary) mass cut, is similar to the radiative process, whereas the QCD component is approximately one hundred times larger, although this can be varied by kinematic selections such as restricting $|\Delta\eta|$. The worse signal-to-background ratio makes the fully-hadronic channel much less promising than the radiative channels for LHC searches. A shift in the W mass peak position in the fully hadronic channel of -970 ± 290 MeV/c^2 was seen.

6. Conclusions

Radiative W boson decays are predicted by PYTHIA and Sherpa for three-body and four-body final states, with branching ratios of a few in 10^{-8}. This is three orders of magnitude below the current sensitivity for the experimentally similar decay of $W^- \to \pi^-\gamma$. It is possible, however, that exclusive hadronic vector boson decays may be observed at the (HL-)LHC. Radiative decays, with a high-energy photon recoiling against a low-multiplicity hadronic system, seem to be the most promising channels.

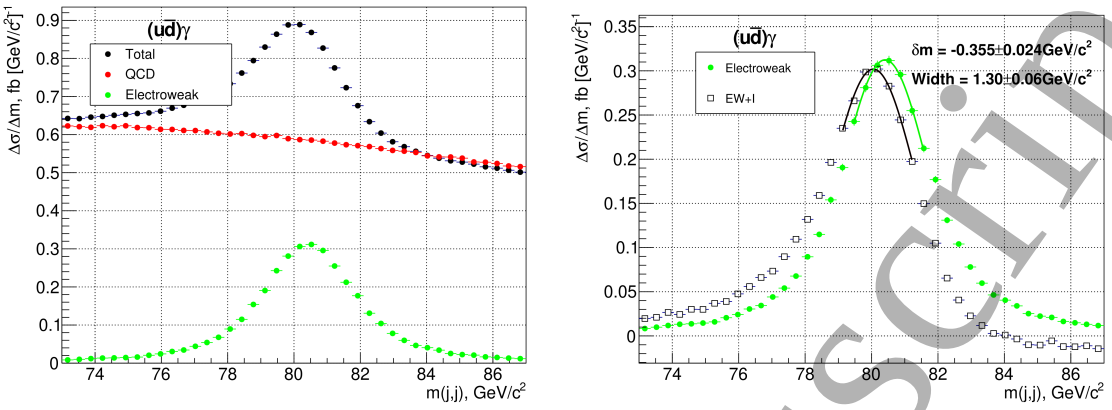

Figure 5. The reconstructed mass peak in the $u\bar{d}\gamma$ system, assuming a 1% detector resolution and requiring the mass of the $u\bar{d}$ system to be below 2 GeV/c^2. Left: the normalised distributions for the EW component (green), QCD component (red) and total (black). Right: A Gaussian fit to the EW (green) and total (black) terms to determine the mass shift.

Although it might be technically feasible to trigger fully-hadronic W boson decays, the poor intrinsic signal-to-background ratio means it is unlikely to be competitive with the radiative decay modes.

In studying such states, three effects need to be understood and controlled: charged hadron misidentification, partial reconstruction and interference. Misidentification is the least significant of these effects; even so, it can produce shifts in the peak mass position of the order of 20 MeV/c^2. The effect of partial reconstruction was found to reduce the peak position by approximately 400 MeV/c^2 for decays to $h^+h^-h^+\gamma$. However, the parton shower simulations have little guidance from data and are close to their kinematic limit, so this prediction must be regarded as unreliable. Interference decreases the measured mass by 300 (100) MeV/c^2 for $u\bar{d}$ ($c\bar{s}$) final states, but it should be noted that these calculations were performed at LO, with no NLO estimate currently available.

All the effects described in this paper can be corrected for; however, uncertainties arising due to effects on the size of the mass shifts will also need to be studied and strategies developed to mitigate them. The effects studied here should also be considered in searches for fully-reconstructed W boson decays.

Acknowledgments

We wish to thank all the referees for their helpful comments and suggestions.

References

[1] Arnellos L, Marciano W and Parsa Z 1982 Radiative Decays: $W^{\pm} \to P^{\pm} + \gamma$ and $Z^0 \to P^0 + \gamma$ *Nucl. Phys. B* **196** 378–393 https://doi.org/10.1016/0550-3213(82)90496-5

[2] Grossman Y, König M and Neubert M 2015 Exclusive radiative decays of W and Z Bosons in QCD factorization *J. High Energy Phys.* **04** JHEP04(2015)101 https://doi.org/10.1007/JHEP04(2015)101

[3] Huang T C and Petriello F 2015 Rare exclusive decays of the Z boson revisited *Phys. Rev. D* **92** 014007 https://doi.org/10.1103/PhysRevD.92.014007

[4] Mangano M and Melia T 2015 Rare exclusive hadronic W decays in a $t\bar{t}$ environment *Eur. J. Phys. C* **75** 258 https://doi.org/10.1140/epjc/s10052-015-3482-x

[5] Keum Y and Pham X Y 1994 Possible huge enhancement in the radiative decay of the weak W boson into a pion or a charmed D_s meson *Mod. Phys. Lett. A* **9** 1545–1556 https://doi.org/10.1142/S0217732394001386

[6] Aaltonen T et al. (CDF Collaboration) 2014 First search for exotic Z boson decays into photons and neutral pions in hadron collisions *Phys. Rev. Lett.* **112** 111803 https://doi.org/10.1103/physrevlett.112.111803

[7] Buskulic D et al. (ALEPH Collaboration) 1992 Searches for new particles in Z decays using the ALEPH detector *Phys. Reports* **216** 253–340 https://doi.org/10.1016/0370-1573(92)90177-2

[8] Abreu P et al. (DELPHI Collaboration) 1998 Measurement of the $e^+e^- \to \gamma\gamma(\gamma)$ cross-section at the LEP energies *Phys. Lett. B* **433** 429–440 https://doi.org/10.1016/S0370-2693(98)00715-1

[9] Aaboud M et al. (ATLAS Collaboration) 2016 Search for Higgs and Z boson decays to $\phi\gamma$ with the ATLAS detector *Phys. Rev. Lett.* **117** 111802 https://doi.org/10.1103/PhysRevLett.117.111802

[10] Aad G et al. (ATLAS Collaboration) 2015 Search for Higgs and Z boson decays $J\psi\gamma$ and $\Upsilon(nS)\gamma$ with the ATLAS detector *Phys. Rev. Lett.* **114** 121801 https://doi.org/10.1103/PhysRevLett.114.121801

[11] Sirunyan A M et al. (CMS Collaboration) 2021 Search for the rare decay of a W boson into a pion and a photon in proton-proton collisions at $\sqrt{s}$ =13 TeV *Phys. Lett. B* **819** 136409 https://doi.org/10.1016/j.physletb.2021.136409

[12] Catani S and Grazzini M 2007 An NNLO subtraction formalism in hadron collisions and its application to Higgs boson production at the LHC *Phys. Rev. Lett.* **98** 222002 https://doi.org/https://doi.org/10.1103/PhysRevLett.98.222002

[13] Catani S et al. 2009 Vector boson production at hadron colliders: a fully exclusive QCD calculation at NNLO *Phys. Rev. Lett.* **103** 082001 https://doi.org/10.1103/PhysRevLett.103.082001

[14] Zyla P A et al. (Particle Data Group) 2020 *Review of Particle Physics* **8** 083C01 https://doi.org/10.1093/ptep/ptaa104

[15] Aaboud M et al. (ATLAS Collaboration) 2018 Search for exclusive Higgs and Z boson decays to $\phi\gamma$ and $\rho\gamma$ with the ATLAS detector *J. High Energy Phys.* **07** 127 https://doi.org/10.1007/JHEP07(2018)127

[16] Chatrchyan S et al. (CMS Collaboration) 2012 Observation of a new boson at a mass of 125 GeV with the CMS experiment at the LHC *Phys. Lett. B* **716** 30–61 https://doi.org/10.1016/j.physletb.2012.08.021

[17] Sjöstrand T, Mrenna S and Skands P 2006 PYTHIA 6.4 physics and manual *J. High Energy Phys.* **05** 026–026 https://doi.org/10.1088/1126-6708/2006/05/026

[18] Sjöstrand T, Mrenna S and Skands P 2008 A brief introduction to PYTHIA 8.1 *Comput. Phys. Comm* **178** 852–867 https://doi.org/10.1016/j.cpc.2008.01.036

[19] Gleisberg T et al. 2009 Event generation with SHERPA 1.1 *J. High Energy Phys.* **02** 007–007 https://doi.org/10.1088/1126-6708/2009/02/007

[20] Schoenherr M and Krauss F 2008 Soft photon radiation in particle decays in SHERPA *J. High*

Energy Phys. **12** 018 https://doi.org/10.1088/1126-6708/2008/12/018

[21] Gleisberg T and Hoeche S 2008 Comix, a new matrix element generator *J. High Energy Phys.* **12** 039 https://doi.org/10.1088/1126-6708/2008/12/039

[22] Bothmann E et al. 2019 Event generation with SHERPA 2.2 *SciPost Phys.* **7** 034 http://dx.doi.org/10.21468/SciPostPhys.7.3.034

[23] Decamp D et al. (ALEPH Collaboration) 1991 Measurement of the charged particle multiplicity distribution in hadronic Z decays *Phys. Lett. B* **273** 181–192 https://doi.org/10.1016/0370-2693(91)90575-B

[24] Ackert A K 2017 Search for Heavy Stable Charged Particles at $\sqrt{s} = 13$ TeV Utilizing a Multivariate Approach CERN-THESIS-2017-082 https://cds.cern.ch/record/2273184.

[25] CMS Collaboration 2019 A MIP Timing Detector for the CMS Phase-2 Upgrade *CERN-LHCC-2019-003, CMS-TDR-020 https://cds.cern.ch/record/2667167*

[26] ATLAS Collaboration 2020 Technical Design Report: A High-Granularity Timing Detector for the ATLAS Phase-II Upgrade *CERN-LHCC-2020-007, ATLAS-TDR-031* https://cds.cern.ch/record/2719855?ln=en

[27] Aad G et al. (ATLAS Collaboration) 2019 Electron and photon performance measurements with the ATLAS detector *JINST* **14** 12006–12006 https://doi.org/10.1088/1748-0221/14/12/p12006

[28] Sirunyan A M et al. (CMS Collaboration) 2020 Electron and photon reconstruction and identification with the CMS experiment at the CERN LHC arXiv:2012.06888 https://arxiv.org/abs/2012.06888

[29] Ranft G and Ranft J 1979 QCD-weak interference and predictions for vector boson signals in hadronic jet cross sections in polarized and unpolarized pp and $\bar{p}p$ collisions *Phys. Lett. B* **87** 122–126 https://doi.org/10.1016/0370-2693(79)90034-0

[30] Baur U, Glover E and Martin A 1989 Electroweak interference effects in two-jet production at pp colliders *Phys. Lett. B* **232** 519–523 https://doi.org/10.1016/0370-2693(89)90452-8

[31] Pumplin J 1992 How to observe hadronic decays of $W^{\pm}$ and Z^0 at hadron colliders *Phys. Rev. D* **45** 806–813 https://doi.org/10.1103/PhysRevD.45.806

[32] Ding C, Fuller B, Jones E, Martin A and Murray W 2020 Electroweak-QCD interference in hadronic vector bosons decays at the LHC *Eur. J. Phys. C* **80** 176 https://doi.org/10.1140/epjc/s10052-020-7729-9